

Power-law statistics and universal scaling are generic features of large ensembles of weakly correlated units

Jonathan Touboul^{1,2,*} and Alain Destexhe^{3,4}

¹*The Mathematical Neuroscience Laboratory, CIRB / Collège de France (CNRS UMR 7241, INSERM U1050, UPMC ED 158, MEMOLIFE PSL*)*

²*MYCENAE Team, INRIA Paris*

³*Unit for Neurosciences, Information and Complexity (UNIC), CNRS, Gif sur Yvette, France*

⁴*The European Institute for Theoretical Neuroscience (EITN), Paris*

(Dated: September 9, 2022)

Power-law scaling is found in many natural systems and is often associated to critical states. We show here analytically and numerically that such statistics emerge naturally in large-scale interacting particle systems with low levels of correlations. Boltzmann's molecular chaos regime, a universal regime, predicts quantitatively these scalings. This shows that the power-law scaling widely found in natural complex systems can be explained statistically, and is a much more general property than criticality.

PACS numbers: 02.50.-r, 05.40.-a, 87.18.Tt, 87.19.ll, 87.19.lc, 87.19.lm

Power-law statistics are ubiquitous in physics and life sciences. They are observed in a wide range of complex phenomena arising in natural systems, from sandpile avalanches to forest fires [1, 2], earthquakes amplitude solar flares, website frequentation as well as economics [3]. Most power-laws are found in collective phenomena built up from the interaction of a large number of elements interacting, in the above examples for instance sand grains, trees or investors, and even earthquake are generally described by many particle systems (see [4]). Using arguments from the renormalization group theory and its universality properties, Sethna and collaborators proposed a unified theory explaining the emergence of power laws in statistical systems. Of crucial importance in this theory, beyond power-law scalings of specific events, is the relationship between the different scaling exponents. Power-law scalings have also been reported in brain recordings, when one considers the statistics of specific events called *neuronal avalanches*, that are periods of collective activity interspersed by silences. First evidences showed power-law scalings of avalanche sizes [5] *in vitro* using indirect evidence of neuronal activity. This finding triggered ample experimental and theoretical work to assess the presence of such statistics and their implication in brain function [6]. A particularly important study in the domain recently reported fine analyzes of actual spikes data recorded *in vitro*, showing the presence of power-law scaling of both avalanche size and duration distributions with exponents consistent with critical systems (namely, $-3/2$ and -2 respectively), as well as a number of additional facts known to be valid for critical systems including the power-law scaling of mean avalanche size with their duration, or scale-invariance of the shape of a neuronal avalanche [7].

In models, power-law scalings have been evidenced in a number of canonical systems such as the Ising model [8] poised at its phase transition; this regime is called critical. At criticality, such systems show a power-law decay of the correlations. The properties of the systems in this regime generally deviate considerably from mean-field properties, and take place in narrow parameter ranges. But specific systems such as the Abelian sandpile [9]

can naturally find their critical state, and this type of mechanism was proposed as a possible origin for power-law scalings in other systems [1], leading to an increased popularity of the criticality assumption in diverse complex systems showing power-law relationships (see [2, 9] for reviews) and related to criticality. So while critical phases are rare, systems may naturally find their critical point through their evolution, and thus display a particular behavior very distinct from mean-field regimes.

Here, we revisit this interpretation of power-law statistics in large-scale systems, and particularly show that power-law scalings with critical exponents may emerge in the mean-field regime. We start by investigating networks of a large number n of interacting units, introduced as a model of neuronal network [10] with excitation and inhibition (see equations, parameters and analysis methods SI Text, section II). Depending on whether inhibition or excitation dominates the network and on the level of external input received by the cells, the network either generates self-sustained *synchronous irregular* (SI) or *asynchronous irregular* (AI) activity states (Fig. 1A,B, respectively, see SI Text II.2). In the AI state, it is not possible to define avalanche dynamics because the activity is sustained. In the SI state, however, the alternation of periods of activity and silences allows the definition of neuronal avalanches. We thus compared the statistics of the avalanches to those of neuronal data [7]. We found that, consistently with neuronal data and with the criticality assumption, the statistics of avalanche size (Fig. 1C) and duration (Fig. 1D) display a statistically significant power-law scaling, with exponents $\tau = 1.42$ and $\alpha = 2.11$ close to the critical $-3/2$ and -2 respectively (see exact statistics and significance levels in Appendix). Also consistent with neuronal data and crackling noise, we found that the average avalanche size scales very clearly as a power of its duration, but with a positive exponent $\gamma = 1.50$, not consistent with the crackling noise relationship between exponents

$$\gamma = \frac{\alpha - 1}{\tau - 1} \quad (1)$$

that predicts an exponent equal to $\gamma = 2.64$, but however quantitatively consistent with the *in vitro* data of [7]. We have also investigated the shape of the avalanches of different durations. We have found that, similarly to

* jonathan.touboul@college-de-france.fr

critical systems or to *in vitro* data, the avalanche shapes collapsed onto a universal scaling function (Fig. 1E) when time is rescaled to a unit interval and shape rescaled by T^γ where γ is the power law exponent of the average size.

Thus, such networks display all features usually attributed to critical systems, but while the scaling exponents were consistent with neuronal data, the power-law scaling of the mean avalanche size did not satisfy the classical scaling relationship between the different exponents in critical systems.

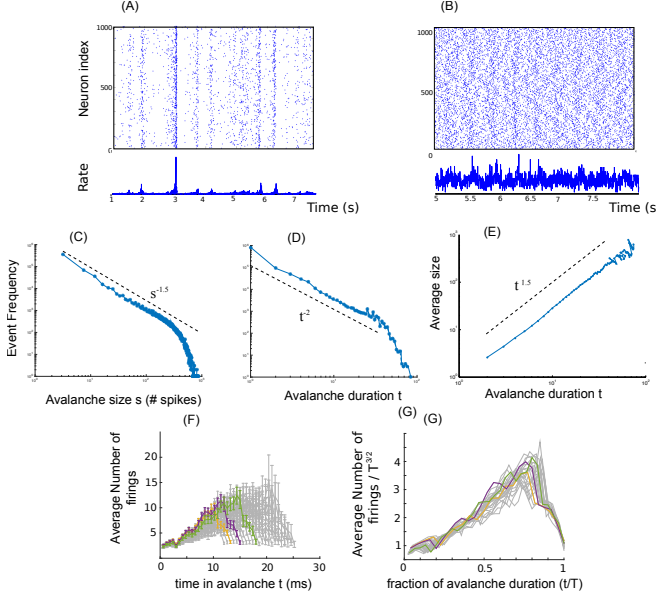


FIG. 1. Avalanche spike statistics in the sparsely connected networks [10] with $N = 5000$ neurons in the SI and AI states. (A) Raster plot of the SI together with the firing rate (below). (B) In the AI state, spiking is asynchronous uninterrupted. In the SI states, (C) avalanche size, (D) avalanche duration and (E) average size of avalanches of a given duration, scale as power-law with exponents consistent with -1.5 , -2 and $+1.5$. Avalanches shapes collapse onto the same curve (F,G) very accurately. See parameters in SI Text II.

All these statistics are thus found within the SI regime of activity of a neuronal network which occurs away from any phase transition of the system, and indeed, the statistics reported in Fig. 1 are valid in a wide region of the parameter space (see supplementary Figure S1). Moreover, the exponential cutoff visible in the tail of the distribution is attributed to finite-size effects and is discussed in more detail in SI Text VI and Supplementary Fig. S2

Rather than being critical, it was shown in [10] that the SI regime satisfies the classical properties of mean-field systems of interacting particles, and in particular that they operate in a the molecular chaos regime. In the large n limit, neurons behave as independent processes but with identical instantaneous firing rates $\nu(t)$. This is a universal phenomenon in the statistical physics of interacting particle systems, historically introduced by Ludwig Boltzmann in the kinetic theory of gases. Boltzmann's molecular chaos (*Stoßzahlansatz*) states that the velocity of colliding particles are uncorrelated and independent of their positions [11]. This property that particles become independent copies of the same statistical process, coined *propagation of chaos property* in mathe-

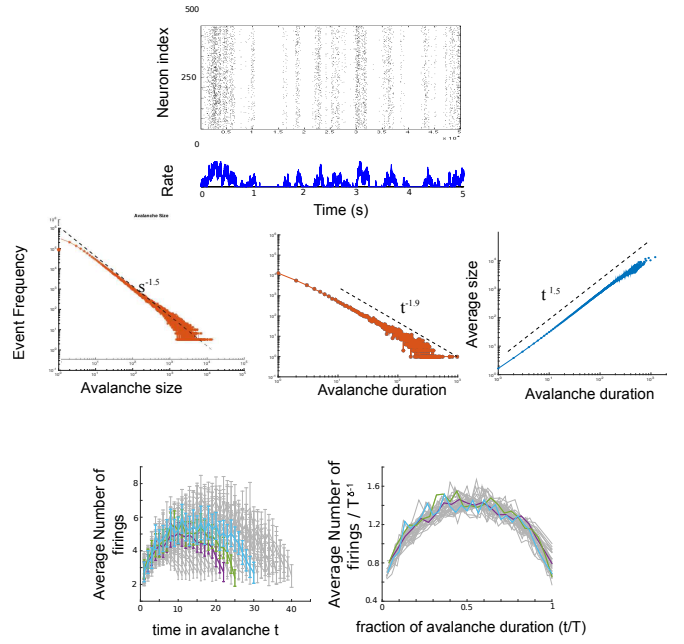


FIG. 2. Avalanches statistics in the independent Poisson model with Ornstein-Uhlenbeck firing rate ($\alpha = \sigma = 1$). Apparent power-law scalings, together with scale invariance of avalanches shapes. Avalanches of size 10 to 40 in gray, 3 specific trajectories highlighted.

matics, has been rigorously demonstrated in various situations and proves extremely general (see, e.g., the review [12] and SI Text IV). This has been in particular explicitly proved in neuronal networks recently [13–15]. This very low correlation level is consistent with recent experimental data in the macaque monkey [16, 17], rodent [18] and human [19] (see details in SI Text V).

We now show that this statistical mechanism provides an alternative natural explanation for the emergence of power-law and scale invariant statistics. To determine if this applies to neuronal avalanches, we designed a surrogate network in which all units were replaced by independent and identically distributed stochastic processes (Fig. 2) with Poisson statistics. In the SI regime, cells display time variable rates with periods of silence occurring irregularly, that we emulated by generating a set of Poisson processes with an irregular common firing rate, chosen for instance by the positive part ρ_t^+ of the Ornstein-Uhlenbeck process:

$$\dot{\rho}_t = -\alpha \rho_t + \sigma \xi_t$$

with (ξ_t) a Gaussian white noise. This choice is interesting in that although periods of silence do not occur periodically, the duration between two such silences have an exponential decay [20].

Interestingly, this stochastic network displayed power-law statistics almost identical to the original network, with scaling exponents close to $-3/2$ for avalanche size and -2 for durations (Fig. 2, middle), yielding a power-law scaling of the mean avalanche size as a function of its duration (with slope 1.4 explaining all the variance but $6 \cdot 10^{-4}$) as well as a very clear collapse of the avalanche shapes onto a universal scaling function (Fig. 2, bottom). We confirmed that these statistics are not related to the

nature of the irregular rate chosen, and show for instance in Supplementary Fig. S3 the avalanche statistics of independent Poisson processes with rate given by the positive part of a reflected Brownian, and we find exactly the same power-law statistics of avalanche shapes and durations, as well as a very nice collapse of avalanche shapes.

In this system, there is no statistical correlation between the different units (they are independent realization of the same stochastic process and thus there is no interaction between the units), although, since they share the same instantaneous firing rate, the firing may seem synchronized. We conclude at this point that power-law statistics and universal scaling exponents are not sufficient to demonstrate criticality.

To further investigate this non-critical origin of power-law theoretically, we have analytically solved the problem under the assumptions that the firing rate $\nu(t)$ is stationary and slow. We fix a time bin dt and note $q(t) = \exp(-\int_t^{t+dt} \nu(s) ds)$ the probability that a neuron does not fire in the interval $[t, t + dt]$ [21]. It is not hard to show that under our hypotheses, denoting ρ the stationary distribution of $q(t)$, that the probability of an avalanche of size τ reads $p_\tau^n = \int_0^1 q^{2n} (1 - q^n)^\tau \rho(q) dq$. As $n \rightarrow \infty$, disregarding all constants and renormalizing the probability, we thus find the universal limit:

$$p_\tau^\infty = \int_0^1 x(1-x)^\tau dx = \frac{1}{(\tau+1)(\tau+2)}$$

which is indeed a power-law with exponent -2 , exactly the one arising in critical systems, consistent with those reported in neuronal data [7], in neuron models (Fig. 1) and in surrogate systems (Fig. 2).

We now show that this extends to the distribution of avalanche size and the scaling of the mean avalanche size with duration. Indeed, the size of avalanches of duration τ have a binomial distribution, corresponding to $s - \tau$ successes among $(n-1)\tau$ independent Bernoulli variables with probability of success $1 - q(t)$. Moreover, De Moivre-Laplace theorem [22] ensures convergence as n increases towards a normal variable with mean $(n-1)\tau p(t)$ and variance $(n-1)\tau p(t)q(t)$ with $p(t) = 1 - q(t)$. Using again our separation of timescale and stationarity hypotheses, we find the probability the probability of finding an avalanche of size s and duration τ averaged on the firing rate:

$$\bar{p}^n(s, \tau) \sim \int_0^1 e^{-\frac{(s-\tau-n(1-q)\tau)^2}{2nq\tau(1-q)}} \frac{q^{2n}(1-q^n)^\tau}{\sqrt{2\pi nq\tau(1-q)}} \rho(q) dq$$

which converges, as $n \rightarrow \infty$, towards:

$$\bar{p}^\infty(s, \tau) \sim \int_0^1 e^{-\frac{(s-\tau(1+\log(u)))^2}{2\tau\log(u)}} \frac{u(1-u)^\tau}{\sqrt{2\pi\tau\log(u)}} du$$

We thus obtain at leading order the size distribution:

$$\mathcal{P}(s) \sim e^s \sum_{\tau=1}^s \int_0^1 e^{\frac{(s-\tau)^2}{2\tau\log(u)}} \frac{u(\sqrt{u}(1-u))^\tau}{\sqrt{2\pi\tau\log(u)}} dx. \quad (2)$$

It is hard to further simplify this formula, but it can be easily evaluated numerically. We depict the result of this computation in Fig. 3 which scales as a power-law with slope $-3/2$.

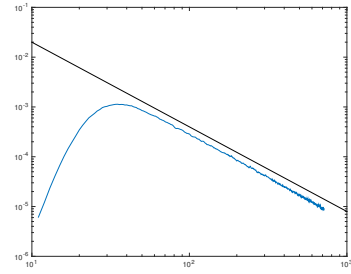


FIG. 3. Universal shape of the avalanche size distribution in the slow rate and large n limit.

Eventually, we obtain for the average size A_τ of avalanches of duration τ :

$$\begin{aligned} A_\tau &\sim \int_0^1 \int_{s=\tau}^\infty s e^{\frac{(s-\tau(1+\log(u)))^2}{2\tau\log(u)}} \frac{ds}{\sqrt{2\pi\tau\log(u)}} du \\ &\sim \tau^{3/2} \int_0^1 (-\log(u))^{5/4} u \sqrt{\frac{\tau}{-8\pi\log(u)}} du. \end{aligned}$$

We thus conclude that while a power-law relationship persists between A_τ and τ , the scaling exponent is not related to the exponents of the power-law of size (3/2) and duration (2) distribution through Sethna's crackling noise relationship, which would predict an exponent equal to 2. Importantly, we note that the exponent found here is quantitatively perfectly consistent with the exponent found in *in vitro* data [7] in the neural network model 1 or surrogate 2.

The analysis of this simple example thus shows that power-law scalings in collective phenomena naturally arise in non-critical systems of independent processes with the same statistics. Moreover, in the case of avalanches, these scalings are identical to critical systems, since exponents $-3/2$ and -2 are found for avalanche size and duration distributions.

We thus conclude that power-law statistics of avalanche duration and size, as well as collapse of avalanche shapes, also arise in non-critical systems, and even in networks in which firing times are statistically independent, as long as the neurons activity is asynchronous (i.e. their firing is statistically independent), but that share correlations in their firing rates. This reveals that power-law statistics do not necessarily a critical regime in which interactions are long-range. Actually, correlations emerging in the collective laws of activity are sufficient to create these power-laws. This new interpretation is thus related to recent findings relating the presence of Zipf's law in statistics in high dimensional data to the presence of latent variables [23, 24] inducing hidden dependences and independence. Here, while the developments and interpretations are very remote [25], the fact that the state of the different particles in our systems are identical can be compared to the presence of a sort of 'hidden' variable, but that naturally from a collective interactions.

The above findings therefore profoundly question the relationship between power-law relationships and criticality in data. At this point, this finding could appear as contradicting a number of outstanding theoretical developments and analyzes showing that only at criticality

power-law relationships appeared [7, 26]. The difference between the models is actually the essential presence of inhibition in our system. Indeed, models with no inhibition mechanism indeed require to propagate activity in average to one other cell to avoid that activity dies out after prescribed time or invade the network. The presence of inhibition can terminate avalanches even in the regime where activity invades the network.

Boltzmann's molecular chaos is a very universal feature in statistical systems. The very particular structure of different particles activity it induces, namely statistical independence of the particles behavior together with a correlation in the law, may induce as we have observed the same type of power-laws as in critical systems, with universal coefficients that are consistent with critical systems. In agreement with this theory, we have seen that the same statistics are reproduced by a sparsely connected network and a surrogate stochastic process where the periods of firing and silences are themselves generated by another stochastic process. Interestingly, a network in Boltzmann's molecular chaos regime can be interpreted as a high dimensional system with a hidden variables, as studied recently in [23, 24]. In these contributions, the authors investigate the rank distribution of high dimensional data with hidden latent variable, and show that such systems display Zipf law scaling (power-laws with slope -1 in the rank distribution) that generically arise from entropy consideration, and using the elegant identity between entropy and energy shown in [27]. While these developments do not generalize here, Boltzmann molecular chaos provides a natural explanation for the emergence of weakly correlated units with similar probability laws: in the neural network system case, the common rate could be seen as a latent variable, and both independence and irregularity build up only from the interactions between cells. As a result of this theory, revealing apparent power-law scaling with exponents of $-3/2$ and 2 , as well as shape collapse, may be entirely explained statistically; in particular, these criteria constitute no proof of criticality and experimental studies solely relying on them should be re-evaluated.

However, as indicated in [4], a prominent characteristic of criticality beyond the presence of power-law scalings is the particular relationship one finds between the exponents. In our study, we have shown that the power-law scalings emerging in the absence of criticality did not satisfy the canonical relationship found in critical systems in [4]. This mismatch should allow to distinguish power-law scalings at criticality from those related to statistical mechanics.

Acknowledgments

A.D. was supported by the CNRS and grants from the European Community (*BrainScales* FP7-269921 and *Human Brain Project* FP7-604102). We warmly thank Quan Shi and Roberto Zúñiga Valladares for preliminary work and analyzes.

Supplementary Information:

We provide here supplementary information and analysis, and describe in detail the methods used in the main text. We start by presenting in section I our techniques to fit power laws to data and to evaluate the statistical significance of the fit. In Fig.1 of the main text, we have investigate the avalanche analysis for a neuronal network model described in supplementary section II. We first review the model used in section II.1 and its different dynamical regimes (section II.2). We then describe in detail the statistical analysis of power-law fits of the avalanches in the model with the parameters of Fig.1 (section II.3), that these scalings persist in the whole region of SI dynamics (section II.4), and investigate finite-size scalings and cutoffs in the power-law scalings in section II.5.

Two neurons in Brunel's models arbitrary low levels of correlation for large network sizes. We discuss in section III whether low levels of correlations may be found in biological neural networks. We review theoretical results on the universality of Boltzmann's molecular chaos regime in section IV. This regime motivated to investigate one particular surrogate in the main text (Figure 2). We provide an alternative surrogate in section V.

I. POWER LAW STATISTICS AND MAXIMUM LIKELIHOOD FITS FOR STATIONARY DATA

We review here the concepts and methods used to fit the power law distributions, that closely follow the methodology exposed in [28]. Taking the logarithm of the probability density of a power-law random variable, we obtain $\log(p(x)) = -\alpha \log(x) + \log(a)$. The histogram of the power-law therefore presents an affine relation in a log-log plot. For this reason, power-laws in empirical data are often studied by plotting the logarithm of the histogram as a function of the logarithm of the values of the random variable, and doing a linear regression to fit an affine line to through the data points (usually using a least-squares algorithm). This method dates back to Pareto in the 19th century (see e.g. [29]). The evaluated point \hat{x}_{\min} corresponding to the point where the data start having a power-law distribution is mostly evaluated visually with possible effects due to noise (see e.g. [30] and references therein). The maximum likelihood estimator of the exponent parameter α corresponding to n data points $x_i \geq x_{\min}$ is:

$$\hat{\alpha} = 1 + n \left(\sum_{i=1}^n \log \frac{x_i}{x_{\min}} \right)^{-1}. \quad (3)$$

The log-likelihood of the data for the estimated parameter value is:

$$L(\hat{\alpha}|X) = n \log \left(\frac{\hat{\alpha} - 1}{x_{\min}} \right) - \hat{\alpha} \sum_{i=1}^n \log \left(\frac{x_i}{x_{\min}} \right).$$

For each lower bound x_{\min} , one can thus compute a power-law exponent and a log-likelihood. We then extract \hat{x}_{\min} by minimizing the Kolmogorov-Smirnov distance:

$$KS = \max_{x \geq x_{\min}} |S(x) - \hat{P}(x)|$$

where $S(x)$ is the cumulative distribution function (CDF) of the data and $\hat{P}(x)$ is the CDF of the theoretical distribution being fitted for the parameter that best fits the data for $x \geq x_{\min}$, as proposed by Clauset and colleagues in [28]. In order to quantify the accuracy of the fit, we use a standard goodness-of-fit test which generates a p-value. This quantity characterizes the likelihood of obtaining a fit as good or better than that observed, if the hypothesized distribution is correct. This method involves sampling the fitted distribution to generate artificial data sets of size n , and then calculating the Kolmogorov-Smirnov distance between each data-set and the fitted distribution, producing the distribution of Kolmogorov-Smirnov distances expected if the fitted distribution is the true distribution of the data. A p-value is then calculated as the proportion of artificial data showing a poorer fit than fitting the observed data set. When this value is close to 1, the data set can be considered to be drawn from the fitted distribution, and if not, the hypothesis might be rejected. The smallest p-values often considered to validate the statistical test are taken between 0.1 and 0.01. These values are computed following the method described in [28], which in particular involves generating artificial samples through a Monte-Carlo procedure.

These methods, very efficient for stationary data, fail to evaluate the tails of non-stationary data as is the case of neuronal data. A weighted Kolmogorov-Smirnov test with a refined goodness of fit estimate valid up to extreme tails [31].

II. AVALANCHES IN SPIKING NETWORK MODELS

We describe here the classical biophysical model of spiking neuronal network with excitatory and inhibitory connections introduced by Brunel in [10] and used in the main text for Figure 1.

II.1. Neuronal network model (Brunel, 2000)

The neural network model we used describes the interaction of n neurons described through their voltage $(v_i)_{i=1 \dots n}$ that decays to reversal potential in the absence of input, receive external input and spikes from interconnected cells, and fire action potentials when the voltage reaches a threshold θ . At crossing the threshold, it is instantaneously reset. In detail, the voltage of neuron i satisfies the equation:

$$\tau \frac{dv_i}{dt} = -v_i + R\tau \sum_{j=1}^n J_{ij} \sum_{k \geq 0} \delta(t - t_j^k - D)$$

while $v_i \leq \theta$, and where the times t_j^k are the firing instants of neuron j , D is the delay, and the coefficients J_{ij} represent the intensity with which a spike from neuron j affects the voltage of neuron i . It is assumed that these coefficients are zero except for a fixed number of cells C with $C/N = \varepsilon \ll 1$ (sparse connectivity) randomly chosen in the network, and the amplitude of the connectivity coefficient J_{ij} are fixed and only depend upon the population of the presynaptic neuron: excitatory (respectively inhibitory) neurons create an instantaneous jump of the

ε	D	J	τ_{rp}	θ	V_r
0.1	1.8 ms	0.2 mV	2 ms	20 mV	10 mV

TABLE I. Parameters used in all simulations of Brunel's model, as in [10].

current of amplitude denoted J (respectively $-gJ$). It is considered that that 80% of all neurons are excitatory, and that 80% of incoming connections to each cell come from excitatory cells. The parameter g is relevant in that it controls the balance between excitation and inhibition: if $g < 4$, the network is dominated by excitation, and otherwise it is dominated by inhibition. The neuron i fires an action potential when v^i reaches a fixed threshold θ , and the depolarization of neuron i is instantaneously reset to a fixed value V_r where it remains fixed during a refractory period τ_{rp} (during this period, the neuron is insensitive to any stimulation). An important parameter is the ratio between the rate of external input ν_{ext} and the quantity denoted ν_{thresh} corresponding to the minimal frequency that can drive one neuron, disconnected from the network, to fire an action potential: $\nu_{thresh} = \frac{\theta}{0.8J\tau}$ (the coefficient 0.8 in that formula corresponds to the fraction of excitatory neurons).

In this model, the parameters that are kept free are the balance between excitation and inhibition g and the external firing rate ν_{ext} . All other parameters are chosen as in table I. For our simulations, we have used the open source algorithm freely available on ModelDB [32, 33].

II.2. Dynamical Regimes of the Brunel model

We summarize the theory developed in [10] and the distinct dynamical regimes found as a function of the parameters. In that paper, the author investigates the different possible dynamical regimes of the network as a function of the parameters ν_{ext} and g using a diffusion approximation and a mean-field analysis, based on the fact that, due to the sparsity of the connectivity, the correlation between neurons decay. This motivates the author to consider the state of the different neurons as considered a collection of independent point processes with the same instantaneous firing rate $\nu(t)$ given by a self-consistent equation. The regime of the network is described as heuristically as follows: during the time interval $[t, t + dt]$, the probability for any given to spike is given by $\nu(t) dt$, and the realization of this random variable are independent in the different neurons. When the rate $\nu(t)$ is constant in time, neurons activate in an asynchronous and irregular manner and the different neurons show no correlation (the AI regime). However, when the rate depends on time, although neurons are independent realizations of the same stochastic process, they tend to activate in a synchronized manner, since the probability that neurons fire are higher at the same time, when $\nu(t)$ reaches a larger value. Such regimes are thus termed *synchronous* in the parlance of [10]. When $\nu(t)$ is periodic, the regime is called synchronous regular (SR), and otherwise synchronous irregular (SI). The analysis of the self-consistent rate equation on the instantaneous firing rate $\nu(t)$ in the mean field limit led to the identification of several regimes that are depicted in Fig. 4:

- The asynchronous irregular (AI) state in which $\nu(t)$ converges towards a strictly positive constant value occurs when the excitatory external input is sufficiently large ($\nu_{ext} > \nu_{thresh}$) and when inhibition dominates excitation ($g > 4$).
- The synchronous regular (SR) regime corresponds to a state in which $\nu(t)$ is a periodic function of time. This regime arises in the excitation dominated regime ($g < 4$). The oscillations frequency is controlled essentially by the transmission delay D and the refractory period τ_{rp} (approximately varying as τ_{rp}/D). The transition thus occurs close from the line $g = 4$.
- The synchronous irregular (SI) regime occurs essentially in the inhibition-dominated regime ($g > 4$) when the input are not sufficient to drive the network to a sustained firing state, i.e. when $\nu_{ext} < \nu_{thresh}$.

II.3. Avalanche statistics in the Brunel model

In Figure 1 of the main text we have plotted the result of the statistical analysis of the Brunel model in the SI state. Panel (A) represents the raster plot with typical avalanches taking place. The distribution of the avalanche size and durations are plotted in logarithmic axes. Strikingly, both avalanche duration and avalanche size show excellent fit to a power law, validated by Kolmogorov Smirnov test of maximum likelihood estimator [28], see summary in section I. We simulated the network for 3 000s with a timestep of 0.1 ms (simulation takes 12 days on Matlab 2015b and was run on 4 separate batches on a macbook pro with processor 2.8 GHz Intel Core i7 and 16 Go of DDR3 RAM memory). The thus obtained raster plot was decomposed into avalanches for binsize equal 0.3 ms, i.e. distinct bins of active firing separated by periods of silence. We have investigate the statistics of these avalanches:

- the avalanche size s , corresponding to the total number of firings during one event, showed a distribution $s^{-\tau}$ with very clear power-law scaling. The exponent computed using the maximum likelihood estimator (3) was $\tau = 1.42$ (Fig.1 (C)). This fit corresponds to a Kolmogorov-Smirnov distance of 0.0097, which gives a very high p-value $p > 0.1$, indicating a statistically significant power-law scaling.
- the avalanche durations t , corresponding to the number of active bins, displays a distribution with a very clear power-law scaling $t^{-\alpha}$. The exponent found with the maximum likelihood estimator (3) was $\alpha = 2.11$ (Fig.1(D)). The Kolmogorov-Smirnov distance with a pure power law is very low (equal to 0.031), and the p-value $p > 0.1$ validated the significance of the power-law distribution for the avalanche duration.
- A significant power-law distribution with slope 1.49 was found in the dependence of the averaged avalanche size as a function of their duration, with a very good fit explaining more than 98% of the variance.

II.4. Independence of the statistics within the SI regime

These scalings are not specific to the particular choice of parameters used in our simulations: we consistently find, in the whole range of parameter values corresponding to the SI state of Brunel's model, and in particular, away from phase transitions, similar apparent power-law scalings with similar scaling exponents. We have reproduced in Fig. 4 the bifurcation diagram [10, Fig.2 B] with the bifurcation lines between AI, SI and SR states. Within the SI state, we have been randomly drawing 30 parameter points and analyzed the avalanches arising for these parameters. We have found that all regimes show a very clear power-law distribution of avalanche size and duration with exponents consistent with the exponents -1.5 and -2 predicted by the theory.

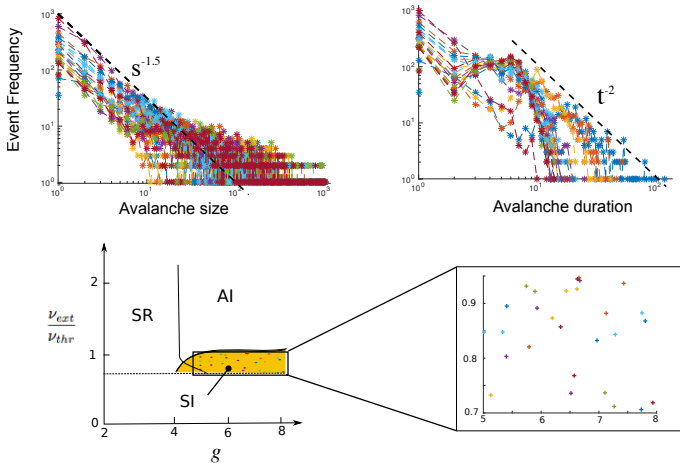


FIG. 4. Avalanche statistics for the Brunel model with randomly chosen parameters within the SI regime.

II.5. Subsampling effects

Of course, any analysis of finite sequences of data is subject to subsampling effects. While these may be neglected for light-tailed data, they become prominent when it comes to assessing possible slow decay of the tails of a statistical sample distribution. These effects were discussed in detail in a number of contributions. In the context of neuronal avalanches, these effects were characterized in [34], and the results show indeed a modification of the slope with subsampling, together with exponential cutoffs pushed to larger sizes as sampling becomes finer.

We have confirmed these results in our own data. In Fig. 5, we have computed the distribution of avalanche size and duration when considering only a fraction of the neurons for the statistics. In detail, we have simulated the Brunel model [10] with $N = 1000$. This yields a raster plot, from which we have extracted a randomly chosen subset of n neurons, with $n = N/k$ for $k \in \{2, 4, 8\}$. We indeed observed that an exponential cutoff is shifted towards larger sizes and slopes increase with the subsampling ratio k .

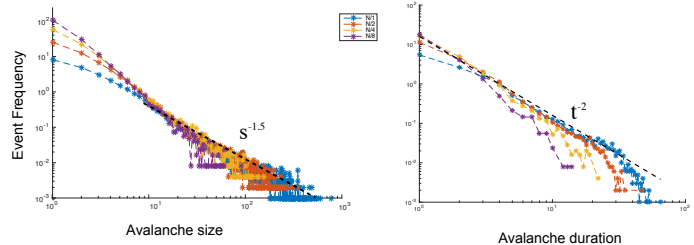


FIG. 5. Subsampling effects. Statistics for a randomly extracted subset of neurons of size $n = 125, 250, 500$ among 1000 neurons whose dynamics is described by Brunel's model. Theoretical power-laws with critical exponents are displayed in black dashed lines.

III. BOLTZMANN MOLECULAR CHAOS IN NATURAL SYSTEMS

In natural environments, regularity of sensory input to the brain may create strong and long-range correlations in space and time [17, 35–38]. It soon appeared that these correlations would be detrimental for the brain to encode sensory stimuli and detect changes efficiently [39, 40]. Theoretical models of the visual system in particular have shown that decrease of redundancy by decorrelation was important for efficient encoding of natural images [41–43]. This was confirmed experimentally. In [19], the authors used high density two-dimensional electrode array and found in particular a marked exponential decay of correlation of excitatory cells in human. A clear confirmation of decorrelation even for closeby cells receiving similar input was recently brought in a remarkable experimental work where chronically implanted multielectrode arrays were developed and implanted in the visual cortex of the macaque [16]. This protocol produced exquisite data allowing to show that even nearby neurons, generally thought to be strongly connected and to receive a substantial part of common input showed a very low level of correlation. Similar decorrelation results were reported in the rodent neocortex [18] with the same level of accuracy.

The origin of this decorrelation is still controversial and several assumptions were formulated, including the role played by adaptation ionic currents that could play central role in temporal decorrelation [44], negative correlations associated with the co-evolution of excitatory and inhibitory cells activity [18], or sophisticated and robust mechanisms relying on neuronal nonlinearities and amplified by recurrent connectivities [45], that was compatible with pattern decorrelation observed in the olfactory bulb of the zebra fish.

All these experimental findings confirm that regimes in which neurons are independent are plausible representations of neural networks activity. We now investigate the avalanche statistics of such networks.

IV. PROPAGATION OF CHAOS IN MATHEMATICAL MODELS

The classical theory of the thermodynamics of interacting particle systems states that in large networks (such as those of the brain), the correlations between neurons vanishes. This is also known as Boltzmann molecular

chaos hypothesis (*Stoßzahlansatz*). In mathematics, this property is called *propagation of chaos*, and is rigorously defined as follows:

Definition 1. For (X_1^n, \dots, X_n^n) a sequence of measures on $(\mathbb{R}^d)^n$. The sequence is said *X-chaotic* if for any $k \in \mathbb{N}$ and i_1, \dots, i_k a set of indexes independent of n , we have $(X_{i_1}^n, \dots, X_{i_k}^n)$ converge to k independent copies of X as $n \rightarrow \infty$.

We refer to [12] for a definition in terms of symmetric probability measures. We note that in contrast with Boltzmann's notion, the mathematical approach generally deals with the independence of any finite subset of neurons, to the notable exception of the work of Ben Arous and Zeitouni [46] who proved propagation of chaos results for subsets of agents of size s_n diverging with n , but such that $s_n/n \rightarrow 0$ as $n \rightarrow \infty$. In our context, in the limit of large networks, neurons behave as independent jump processes with a common rate, which is solution of an implicit equation. This property is at the core of theoretical approaches to understand the dynamics of large-scale networks [10, 47–49]. In the case of Brunel's model, it is shown that since two neurons share a vanishing proportion of common input in the thermodynamic limit, allowing to conclude that the correlation of the fluctuating parts of the synaptic input of different neurons are negligible. This leads the authors to conclude that the spike trains of different neurons are independent point processes with an identical instantaneous firing rate $\nu(t)$ that is solution of a self-consistent equation (see [10, p. 186, first column]). In that view, except in the case of constant firing rate (the asynchronous irregular state), neurons always show a certain degree of synchrony due to the correlations of the instantaneous firing rates of different neurons.

Mathematically, several methods were developed for interacting particle systems and gases (see e.g. [12] for an excellent review). It is shown that generically, systems of interacting agents, with sufficient regularity, show propagation of chaos. It is worth mentioning a remarkable result by Ben Arous and Zeitouni who extended this result to an infinite set of elements (up to \sqrt{n}) [46]. All these results are in particular valid for neuronal networks, as was shown recently in a number of distinct situations. Large n limits and propagation of chaos was demonstrated for large networks of integrate-and-fire neurons [13, 15, 50], firing-rate models with multiple populations [51], for conductance-based models even in the large time regime [52], and was shown to hold in realistic network models incorporating delays and the spatial extension of the system [14, 53]. All the results can be essentially stated in the following form. All different models of large neuronal networks of size n describe the activity x^i of a neuron i through a stochastic differential equation, possibly in random environment (when considering heterogeneous cells or interconnections). Convergence results on the activity of the network consists mostly in showing convergence of an abstract object, the *empirical measure* of the system:

$$\hat{\mu}_n = \frac{1}{n} \sum_{j=1}^n \delta_{x_j}.$$

The methods used to show convergence of this object depend on the specific model chosen; in neuroscience, they

include from coupling methods [50, 53], compacity estimates [13] or large deviations [54]. This convergence is sufficient to show propagation of chaos. Indeed, a very powerful and universal mathematical result demonstrated in [55, Lemma 3.1] ensures that the convergence of the empirical measure of a particle systems towards a unique measure implies propagation of chaos, or in the formulation of [12]:

Theorem 1. (X_1^n, \dots, X_n^n) is *X-chaotic* if and only if their empirical measure converges in law towards the constant random variable X .

All these results and applications to neural networks that we reviewed here indicate that a universal form of activity emerges from neural networks, whereby neurons are independent copies of the same process. Before investigating the avalanche statistics of such regimes of activity, let us discuss the plausibility of the existence of these regimes in neuronal data.

V. DIVERSE REGIMES OF INDEPENDENT PROCESSES

We have confirmed that the statistics of independent Poisson processes with fluctuating instantaneous firing rates produce avalanches with power-law distributions of

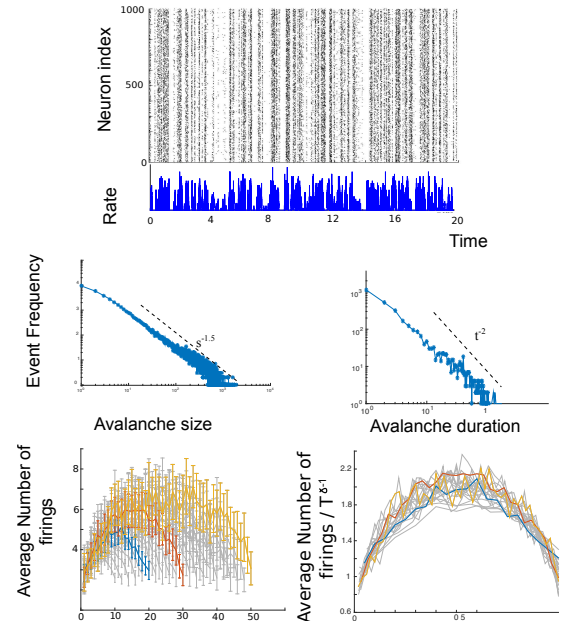


FIG. 6. Avalanche statistics and shape collapses for independent Poisson processes with rates given by a reflected Brownian motion.

avalanche size and durations, consistent with our theory. To this purpose, we have performed a similar analysis as in Fig.2 (main text) replacing Ornstein-Uhlenbeck firing rates by the positive part of a Brownian motion reflected at ± 1 . This choice was motivated by two constraints: the positive part was taken in order to consider only positive firing rates for consistency, and the reflection at ± 1 was forced in order to prevent from having to long excursions of the Brownian motion, so that we can indeed

assess that the heavy tails of the avalanche distributions are rather due to the statistical structure of the firings rather than due to possible very long excursions of the Brownian motion. The results of the simulations are provided in Fig. 6. As in the case of the positive part of the

Ornstein Uhlenbeck process, we find very clear power-law distributions of avalanche size and durations, with slopes consistent with our theory, and a very clear collapse of the avalanche shapes.

[1] P. Bak, *How nature works* (Oxford university press Oxford, 1997).

[2] H. J. Jensen, *Self-organized criticality: emergent complex behavior in physical and biological systems*, Vol. 10 (Cambridge university press, 1998).

[3] M. E. Newman, *Contemporary physics* **46**, 323 (2005).

[4] J. P. Sethna, K. A. Dahmen, and C. R. Myers, *Nature* **410**, 242 (2001).

[5] J. M. Beggs and D. Plenz, *The Journal of neuroscience* **23**, 11167 (2003).

[6] W. L. Shew and D. Plenz, *The neuroscientist* **19**, 88 (2013).

[7] N. Friedman, S. Ito, B. A. Brinkman, M. Shimono, R. L. DeVille, K. A. Dahmen, J. M. Beggs, and T. C. Butler, *Physical review letters* **108**, 208102 (2012).

[8] M. Kardar, *Statistical physics of fields* (Cambridge University Press, 2007).

[9] P. Bak, C. Tang, K. Wiesenfeld, *et al.*, *Physical review letters* **59**, 381 (1987).

[10] N. Brunel, *Journal of computational neuroscience* **8**, 183 (2000).

[11] L. Boltzmann, *Lectures on gas theory* (Univ of California Press, 1964).

[12] A. Sznitman, *Ecole d'Eté de Probabilités de Saint-Flour XIX* , 165 (1989).

[13] P. Robert and J. D. Touboul, *arXiv preprint arXiv:1410.4072* (2014).

[14] J. Touboul *et al.*, *The Annals of Applied Probability* **24**, 1298 (2014).

[15] F. Delarue, J. Inglis, S. Rubenthaler, E. Tanré, *et al.*, *The Annals of Applied Probability* **25**, 2096 (2015).

[16] A. Ecker, P. Berens, G. Keliris, M. Bethge, N. Logothetis, and A. Tolias, *science* **327**, 584 (2010).

[17] E. Zohary, M. N. Shadlen, and W. T. Newsome, (1994).

[18] A. Renart, J. De la Rocha, P. Bartho, L. Hollender, N. Parga, A. Reyes, and K. Harris, *science* **327**, 587 (2010).

[19] A. Peyrache, N. Dehghani, E. N. Eskandar, J. R. Madsen, W. S. Anderson, J. A. Donoghue, L. R. Hochberg, E. Halgren, S. S. Cash, and A. Destexhe, *Proceedings of the National Academy of Sciences* **109**, 1731 (2012).

[20] L. Alili, P. Patie, and J. L. Pedersen, *Stochastic Models* **21**, 967 (2005).

[21] It is clear that the approach works for a more general system of n interacting agents described by a Cox point process.

[22] W. Feller, *An introduction to probability theory and its applications*, Vol. 2 (John Wiley & Sons, 2008).

[23] D. J. Schwab, I. Nemenman, and P. Mehta, *Physical review letters* **113**, 068102 (2014).

[24] L. Aitchison, N. Corradi, and P. E. Latham, *arXiv preprint arXiv:1407.7135* (2014).

[25] In these references, frequency of events are studied in systems with hidden correlations and are proved using a very elegant identity between the entropy and the energy only valid for Zipf law with slope -1 and proved in [27].

[26] A. Levina, J. M. Herrmann, and T. Geisel, *Physical review letters* **102**, 118110 (2009).

[27] T. Mora and W. Bialek, *Journal of Statistical Physics* **144**, 268 (2011).

[28] A. Clauset, C. R. Shalizi, and M. E. Newman, *SIAM review* **51**, 661 (2009).

[29] B. C. Arnold, *Pareto distribution* (Wiley Online Library, 1985).

[30] S. A. Stoev, G. Michailidis, and M. S. Taqqu, *arXiv preprint math/0609163* (2006).

[31] R. Chicheportiche and J.-P. Bouchaud, *Physical Review E* **86**, 041115 (2012).

[32] M. L. Hines, T. Morse, M. Migliore, N. T. Carnevale, and G. M. Shepherd, *Journal of Computational Neuroscience* **17**, 7 (2007).

[33] M. Migliore, T. Morse, A. P. Davison, L. Marenco, G. M. Shepherd, and M. L. Hines, *Neuroinformatics* **1**, 135 (2003).

[34] V. Priesemann, M. H. Munk, and M. Wibral, *BMC neuroscience* **10**, 40 (2009).

[35] D. L. Ruderman, *Network: computation in neural systems* **5**, 517 (1994).

[36] D. L. Ruderman and W. Bialek, *Physical review letters* **73**, 814 (1994).

[37] D. W. Dong and J. J. Atick, *Network: Computation in Neural Systems* **6**, 159 (1995).

[38] Y. Dan, J. J. Atick, and R. C. Reid, *The Journal of Neuroscience* **16**, 3351 (1996).

[39] F. Attneave, *Psychological review* **61**, 183 (1954).

[40] H. B. Barlow, (1961).

[41] S. Laughlin, *Z Naturforsch* **36**, 910 (1981).

[42] E. P. Simoncelli and B. A. Olshausen, *Annual review of neuroscience* **24**, 1193 (2001).

[43] A. Dimitrov and J. D. Cowan, *Neural computation* **10**, 1779 (1998).

[44] X.-J. Wang, Y. Liu, M. V. Sanchez-Vives, and D. A. McCormick, *Journal of neurophysiology* **89**, 3279 (2003).

[45] M. T. Wiechert, B. Judkewitz, H. Riecke, and R. W. Friedrich, *Nature neuroscience* **13**, 1003 (2010).

[46] G. Ben Arous and O. Zeitouni, in *Annales de l'IHP Probabilités et statistiques*, Vol. 35 (1999) pp. 85–102.

[47] A. Renart, N. Brunel, and X.-J. Wang, *Computational neuroscience: A comprehensive approach* , 431 (2004).

[48] H. Sompolinsky, A. Crisanti, and H. Sommers, *Physical Review Letters* **61**, 259 (1988).

[49] S. Ostojic, *Nature neuroscience* **17**, 594 (2014).

[50] N. Fournier and E. Löcherbach, *arXiv preprint arXiv:1410.3263* (2014).

[51] J. Touboul, G. Hermann, and O. Faugeras, *SIAM Journal on Applied Dynamical Systems* **11**, 49 (2012).

[52] S. Mischler, C. Quininao, and J. Touboul, *arXiv preprint arXiv:1503.00492* (2015).

[53] J. Touboul, *Journal of Statistical Physics* **156**, 546 (2014).

[54] T. Cabana and J. Touboul, *Journal of Statistical Physics* **153**, 211 (2013).

[55] A.-S. Sznitman, *Journal of functional analysis* **56**, 311 (1984).